



## Operation Loss Minimization Targeted Distributed Optimal Control of DC Microgrids

Fan, Zhen; Fan, Bo; Peng, Jiangkai; Liu, Wenxin

*Published in:*  
IEEE Systems Journal

*DOI (link to publication from Publisher):*  
[10.1109/JSYST.2020.3035059](https://doi.org/10.1109/JSYST.2020.3035059)

*Publication date:*  
2021

*Document Version*  
Accepted author manuscript, peer reviewed version

[Link to publication from Aalborg University](#)

*Citation for published version (APA):*  
Fan, Z., Fan, B., Peng, J., & Liu, W. (2021). Operation Loss Minimization Targeted Distributed Optimal Control of DC Microgrids. *IEEE Systems Journal*, 15(4), 5186 - 5196. <https://doi.org/10.1109/JSYST.2020.3035059>

### General rights

Copyright and moral rights for the publications made accessible in the public portal are retained by the authors and/or other copyright owners and it is a condition of accessing publications that users recognise and abide by the legal requirements associated with these rights.

- Users may download and print one copy of any publication from the public portal for the purpose of private study or research.
- You may not further distribute the material or use it for any profit-making activity or commercial gain
- You may freely distribute the URL identifying the publication in the public portal -

### Take down policy

If you believe that this document breaches copyright please contact us at [vbn@aub.aau.dk](mailto:vbn@aub.aau.dk) providing details, and we will remove access to the work immediately and investigate your claim.

# Operation Loss Minimization Targeted Distributed Optimal Control of DC Microgrids

Zhen Fan, *Student Member, IEEE*, Bo Fan <sup>id</sup>, *Member, IEEE*, Jiangkai Peng, *Student Member, IEEE*, and Wenxin Liu <sup>id</sup>, *Senior Member, IEEE*

**Abstract**—DC microgrids are growing in popularity due to their advantages in terms of simplicity and energy efficiency while connecting dc sources and dc loads. In traditional hierarchical schemes, optimization and control are implemented at different time scales. The loose integration lowers its energy efficiency and makes it hard to achieve real-time optimization. Even a slight disturbance can result in deviations of bus voltages and output currents from their optimal operating points. Additionally, most real-time control schemes cannot guarantee the boundedness of individual bus voltages. Targeting these problems, a distributed optimal control algorithm is presented in this article for dc microgrids to minimize operation loss (converter loss and distribution loss) in real time and maintain all bus voltages within predefined ranges. First, the Karuch–Kuhn–Tucker condition of the original constrained optimization problem is converted to an equivalent optimality condition, which is suitable for control design. Then, a distributed control algorithm is designed to drive the system’s operating condition toward the optimal one. Convergence to the optima is guaranteed through rigorous Lyapunov-based stability analyses. Finally, simulation studies with a detailed switch-level model demonstrate the merits of the proposed controller.

**Index Terms**—DC microgrids, distributed control, Lyapunov analysis, operation loss optimization, optimal control.

## NOMENCLATURE

$\alpha$	User-defined positive constant.
$a_i$	Converter loss quadratic coefficient of DG $i$ .
$b_i$	Converter loss linear coefficient of DG $i$ .
$C$	Total operation loss.
$C_{\text{conv}_i}$	Converter loss of DG $i$ .
$C_{\text{dis}}$	Distribution loss.
$c_i$	Converter loss constant of DG $i$ .
$\eta$	Vector of partial derivatives of converter loss.
$\eta_i$	Partial derivative of converter loss.
$\mathcal{E}_C$	Set of edges of graph $\mathcal{G}_C$ .
$\mathcal{E}_E$	Set of edges of graph $\mathcal{G}_E$ .
$\mathcal{G}_C$	Graph of the communication network.

$\mathcal{G}_E$	Graph of the electrical network.
$\mathbf{G}$	Nodal admittance matrix.
$G_{ij}$	Element in the $i$ th row and $j$ th column of $\mathbf{G}$ .
$g_{ij}$	Conductance of the distribution line between DG $i$ and DG $j$ .
$\mathbf{I}$	Output current vector.
$\hat{\mathbf{I}}$	Vector of the internal current control signal.
$I_i$	Output current of DG $i$ .
$\hat{I}_i$	Internal current control signal of DG $i$ .
$\bar{I}_i$	Output current upper bound of DG $i$ .
$\underline{I}_i$	Output current lower bound of DG $i$ .
$\mathbf{I}_L$	Load current vector.
$I_{Li}$	Load current of bus $i$ .
$\mu$	Integral of the current error vector.
$\mu_i$	Integral of the current error of DG $i$ .
$n$	Number of DGs.
$\Omega_I$	Set constraint of the current.
$\Omega_V$	Set constraint of the voltage.
$\mathcal{V}_C$	Set of nodes of graph $\mathcal{G}_C$ .
$\mathcal{V}_E$	Set of nodes of graph $\mathcal{G}_E$ .
$\mathbf{V}$	Bus voltage vector of DGs.
$V_i$	Bus voltage of DG $i$ .
$\bar{V}_i$	Bus voltage upper bound of DG $i$ .
$\underline{V}_i$	Bus voltage lower bound of DG $i$ .
$V_{i\_ref}$	Bus voltage reference of DG $i$ .

## I. INTRODUCTION

**M**ICROGRIDS and distributed generations (DGs) have advantages in terms of flexibility and capability in addressing growing consumer demands. Since many renewable generations, energy storage systems, and modern loads are dc by nature [1], [2], it is desirable to deploy a dc microgrid to eliminate the unnecessary ac–dc and dc–ac conversion stages [3]. Since dc microgrids do not have issues like frequency synchronizations and reactive power [4]–[8], it is less technically challenging to control compared to ac microgrids [9]–[11]. Hence, dc microgrids are growing in popularity, especially for some special high-performance applications. However, dc microgrids are hard to control due to their low inertia, large uncertainties, and a wide range of operations [12].

To control a dc microgrid composed of multiple DGs, centralized hierarchical control schemes are usually deployed [13], [14], which can lower design complexity through time-scale

Manuscript received May 3, 2020; revised September 14, 2020; accepted October 20, 2020. This work was supported by the U.S. Office of Naval Research under Grant N00014-18-1-2185. (Corresponding author: Bo Fan.)

Zhen Fan, Jiangkai Peng, and Wenxin Liu are with the Smart Microgrid and Renewable Technology Research Laboratory, Department of Electrical and Computer Engineering, Lehigh University, Bethlehem, PA 18015 USA (e-mail: zhf217@lehigh.edu; jip216@lehigh.edu; wliu@lehigh.edu).

Bo Fan is with the Department of Energy Technology, Aalborg University, Aalborg 9220, Denmark (e-mail: bof@et.aau.dk).

Digital Object Identifier 10.1109/JSYST.2020.3035059

separation. In these schemes, operation loss optimization and real-time control are performed to improve energy efficiency and ensure system stability, respectively. However, the centralized structure lacks flexibility and is susceptible to a single point of failure [15].

To improve the reliability, flexibility, and scalability of dc microgrids, many distributed control algorithms, i.e., each DG's controller only communicates with its neighbors', are developed for dc microgrids over the past decade [16]–[19]. These algorithms are usually designed based on consensus techniques [20]–[23] to realize proportional load sharing and global average bus voltage regulation [24]–[26]. However, since only the average bus voltage is regulated, some bus voltage(s) may become dangerously high or low, which could damage vital and sensitive loads. To solve this problem, Han *et al.* [27] developed a compromised distributed controller to achieve proportional current sharing and bounded bus voltage regulation, where individual bus voltages can be contained in their boundaries tightly. However, operational cost is not considered in these consensus-based distributed algorithms.

To enhance energy efficiency and reliability, distributed optimizations are implemented for dc microgrids to minimize the operation loss [28]–[30]. Nevertheless, optimization and control are performed at different time scales in these methods, which makes it hard to realize real-time optimization in dc microgrids [31]. This is mainly because the optimization is implemented periodically to obtain the optimal bus voltage or output current references for given operating conditions [32], which will unavoidably deviate from the actual ones. Even slight disturbances such as load changes will trigger real-time control adjustments. The consequence is that the bus voltages and output currents will not be optimal even if their references are optimized and updated periodically. Hence, the overall cost will be increased due to the disconnection between optimization and real-time control. To overcome this issue, it is preferable to solve the optimization problem through real-time control directly. Additionally, if voltage bounds are formulated into the optimization problem, the optimal solution can automatically guarantee all bus voltages being bounded. Moreover, compared to ac microgrids, such optimization problems in dc microgrids are relatively simple, making it possible to realize these challenging objectives.

Based on the above analysis, it is preferable to design real-time control that dynamically drives the dc microgrid toward the optimal operating condition, i.e., optimal control strategies to minimize the total generation or operational costs under constraints. In recent years, there appear a few studies that try to realize optimal control for dc microgrids based on convex optimization theory [33]–[35]. In [33], the generation cost for a one-bus system is optimized. A convex optimization problem is formulated with generation constraints, which is further solved by combining the equal increment rate criteria and a subgradient algorithm. Besides, the developed method can achieve proportional power sharing among DGs. Further, the convex generation cost optimization problem for a multiple-bus dc microgrid is solved based on distributed consensus algorithms [34]. The average bus voltage regulation is also achieved. Nevertheless, the aforementioned solutions [33], [34] lack individual bus voltage

regulation capability. To deal with this issue, Wang *et al.* [35] proposed a unified distributed control scheme for dc microgrids with generation and individual bus voltage constraints. This approach can dynamically make the operating conditions converge to the optimal one. However, it requires real-time load information, which is hard to be obtained in dc microgrids. Also, a lot of information has to be exchanged among the distributed controllers. The communication burden is increased. Furthermore, although these designs can respond to the changing operating conditions, the closed-loop system stability analysis is not provided rigorously.

To this end, a distributed optimal control algorithm is presented in this article to minimize the total operation loss (converter loss and distribution loss). At the outset, a convex optimization problem is formulated with bus voltage and output current constraints. By utilizing the Karush-Kuhn-Tucker (KKT) condition and the project operator, an equivalent optimality condition of the original optimization problem is derived to help the distributed control design. Next, a distributed optimal control algorithm for dc microgrids is developed to dynamically find and realize the optimal solution in real time. Each local controller only requires local and its neighbors' lumped information. Thereafter, rigorous stability and convergence analyses based on Lyapunov synthesis are offered. Detailed switch-level simulations are conducted to validate the effectiveness of the proposed distributed optimal control algorithm. The main contributions of this article are summarized as follows.

- 1) A distributed optimal control method for dc microgrids is presented, which can respond quickly to load changes and dynamically minimize the operation loss online under constraints.
- 2) An equivalent optimality condition for the operation loss optimization problem is derived, which aids the development of real-time control schemes.
- 3) The individual bus voltage regulation is guaranteed theoretically during both the transient- and steady-state to ensure secure operation and improve system reliability and power quality.
- 4) Only a lumped variable is required to be transmitted to the neighbors of a DG through the communication network. The communication burden of the entire system is reduced due to the limited information exchange.
- 5) The closed-loop system stability and convergence analyses are performed theoretically. The bus voltages and output currents will converge to their optimal/optimum asymptotically.

The rest of this article is organized as follows. Section II illustrates the model of the considered dc microgrid. In Section III, the operation loss optimization problem as well as the original and equivalent optimality conditions is introduced. Afterward, the distributed optimal control algorithm is developed in Section IV. Main results including the stability and convergence of the proposed algorithm and the individual bus regulation performance are demonstrated in Section V. In Section VI, simulation results are offered to showcase the merits of the proposed algorithms. Finally, Section VII concludes this article.

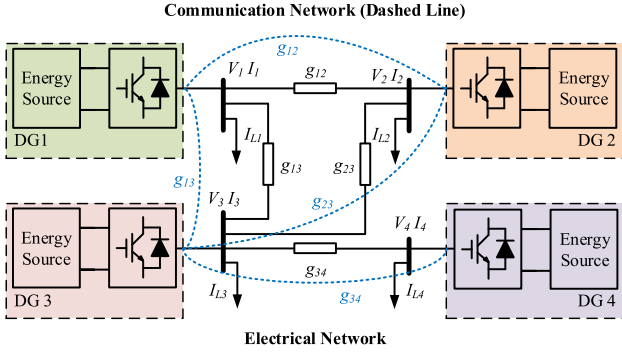


Fig. 1. Model of a dc microgrid.

## II. DC MICROGRID MODELING

Fig. 1 presents the model of a dc microgrid composed of an electrical network (solid line) and a communication network (dashed line). The former is a physical grid for delivering electric power from DGs to loads, while the latter is a sparse network for information sharing among the DGs' distributed controllers [22]. The energy source is connected to the electrical network through a dc-dc or ac-dc converter. Since the distribution lines are predominantly resistive in dc microgrids, the dynamic effects of the line inductance and capacitance are therefore neglected [21], [22].

### A. Electrical Network Modeling of DC Microgrids

The electrical network model of a dc microgrid can be treated as an undirected and connected graph  $\mathcal{G}_E = (\mathcal{V}_E, \mathcal{E}_E)$ , where the set  $\mathcal{V}_E = \{1, 2, \dots, n\}$  denotes the  $n$  buses with DGs and possible load connections, and the set  $\mathcal{E}_E \subseteq \mathcal{V}_E \times \mathcal{V}_E$  denotes the distribution lines. The nodal admittance matrix is then defined as  $\mathbf{G} = \{G_{ij}\} \in \mathbb{R}^{n \times n}$  with its entries given as

$$G_{ij} = \begin{cases} \sum_{m=1, m \neq i}^n g_{im}, & i = j \\ -g_{ij} & i \neq j \end{cases} \quad (1)$$

where  $g_{ij} = g_{ji} \in \mathbb{R}^+$  is the conductance of the distribution line between bus  $i$  and bus  $j$  if  $(i, j) \in \mathcal{E}_E$ , and  $g_{ij} = g_{ji} = 0$  otherwise. Note that  $\mathbf{G}$  is also the Laplacian matrix of graph  $\mathcal{G}_E$  [36].

Next, according to Kirchhoff's current law (KCL), one has

$$I_i = \sum_{j=1}^n g_{ij}(V_i - V_j) + I_{L_i} = \sum_{j=1}^n G_{ij}V_j + I_{L_i} \quad (2)$$

where  $I_i \in \mathbb{R}$  denotes the output current of DG  $i$ , and  $V_i \in \mathbb{R}$  and  $I_{L_i} \in \mathbb{R}$  denote the voltage and load current of bus  $i$ , respectively. Rewriting (2) in a compact form yields

$$\mathbf{I} = \mathbf{G}\mathbf{V} + \mathbf{I}_L \quad (3)$$

where  $\mathbf{V} = [V_1, V_2, \dots, V_n]^T \in \mathbb{R}^n$ ,  $\mathbf{I} = [I_1, I_2, \dots, I_n]^T \in \mathbb{R}^n$ , and  $\mathbf{I}_L = [I_{L1}, I_{L2}, \dots, I_{Ln}]^T \in \mathbb{R}^n$ .

### B. Communication Network Modeling of DC Microgrids

As illustrated in Fig. 1, the communication network among the DGs' controllers can also be considered as an undirected and connected graph  $\mathcal{G}_C = (\mathcal{V}_C, \mathcal{E}_C)$  with the set  $\mathcal{V}_C = \{1, 2, \dots, n\}$  denoting the  $n$  distributed controllers and the set  $\mathcal{E}_C \subseteq \mathcal{V}_C \times \mathcal{V}_C$  denoting the communication links among the controllers. In this article, the communication network is designed to be identical to the electrical one, i.e.,  $\mathcal{G}_C = \mathcal{G}_E$ , as shown in Fig. 1. Hence, the Laplacian matrix of graph  $\mathcal{G}_C$  is also identical to the nodal admittance matrix  $\mathbf{G}$ .

## III. OPERATION LOSS OPTIMIZATION OF DC MICROGRIDS

In this section, the operation loss optimization problem of dc microgrids is introduced. Furthermore, a necessary and sufficient condition for the optimal solution to the problem is derived, which aids the design of the distributed optimal control law in Section IV.

### A. Operation Loss Optimization Problem Formulation

To improve energy efficiency, the operation loss including the distribution loss and converter loss should be minimized [14], which can be formulated as the following convex optimization problem:

$$\begin{aligned} \min_{\mathbf{V}, \mathbf{I}} C(\mathbf{V}, \mathbf{I}) &= C_{\text{dis}}(\mathbf{V}) + \sum_{i=1}^n C_{\text{conv}_i}(I_i) \\ \text{s.t.} & \quad (3) \\ & \underline{V}_i \leq V_i \leq \bar{V}_i, i \in \mathcal{V}_E \\ & \underline{I}_i \leq I_i \leq \bar{I}_i, i \in \mathcal{V}_E \end{aligned} \quad (4)$$

where  $C_{\text{dis}}(\bullet) : \mathbb{R}^n \rightarrow \mathbb{R}$  and  $C_{\text{conv}_i}(\bullet) : \mathbb{R} \rightarrow \mathbb{R}$ ,  $i \in \mathcal{V}_E$  are continuous convex functions, and  $C_{\text{dis}}(\mathbf{V})$  denotes the total distribution loss, i.e., the power loss of the distribution lines which is expressed as [14]

$$C_{\text{dis}}(\mathbf{V}) = \mathbf{V}^T \mathbf{G} \mathbf{V}. \quad (5)$$

$C_{\text{conv}_i}(I_i)$  is the  $i$ th DG's converter loss and can be expressed as the following quadratic function of the output current  $I_i$  [14], [37]:

$$C_{\text{conv}_i}(I_i) = a_i I_i^2 + b_i |I_i| + c_i \quad (6)$$

where  $a_i, b_i$ , and  $c_i \in \mathbb{R}^+$  are constant converter loss coefficients. Hence,  $C(\bullet) : \mathbb{R}^{2n} \rightarrow \mathbb{R}$  stands for the total operation loss of the dc microgrid.  $\underline{V}_i \in \mathbb{R}$  and  $\bar{V}_i \in \mathbb{R}$  are the  $i$ th DG's bus voltage lower and upper bounds, respectively, which are formulated to ensure the secure operation of dc microgrids.  $\underline{I}_i \in \mathbb{R}$  and  $\bar{I}_i \in \mathbb{R}$  are the  $i$ th DG's output current lower and upper bounds determined by the DG's capacity.

*Assumption 1:* Slater's constraint qualification condition [38] holds, i.e., there exists an interior point  $\tilde{\mathbf{V}} \in \Omega_{\mathbf{V}}$ ,  $\tilde{\mathbf{I}} \in \Omega_{\mathbf{I}}$  such that  $\tilde{\mathbf{I}} = \mathbf{G}\tilde{\mathbf{V}} + \mathbf{I}_L$ , where  $\Omega_{\mathbf{V}} = \{\mathbf{V} \in \mathbb{R}^n | \underline{V}_i \leq V_i \leq \bar{V}_i, i \in \mathcal{V}_E\}$ ,  $\Omega_{\mathbf{I}} = \{\mathbf{I} \in \mathbb{R}^n | \underline{I}_i \leq I_i \leq \bar{I}_i, i \in \mathcal{V}_E\}$ .

Note that  $\Omega_{\mathbf{I}}$  and  $\Omega_{\mathbf{V}}$  are both convex sets. The equality constraint is affine. Since  $\nabla^2 C = \text{diag}(\mathbf{G}, \mathbf{A})$  with  $\mathbf{G} \geq 0$  and  $\mathbf{A} = \text{diag}(a_1, \dots, a_n) > 0$ , the cost function  $C(\mathbf{V}, \mathbf{I})$  is also convex. Thus, the optimization problem is convex.

Before the design of optimal control algorithms, the control objective, i.e., the optimal solution to the problem (4), is required. With the help of Assumption 1, the necessary and sufficient condition for the optimal solution to the problem (4) is stated in the following lemma, which is known as the KKT condition [38].

*Lemma 1:* With Assumption 1,  $(\mathbf{V}^*, \mathbf{I}^*)$  is an optimal solution to problem (4) if and only if there exist  $\boldsymbol{\mu}^* \in \mathbb{R}^n$  such that

$$(\mathbf{V} - \mathbf{V}^*)^T \mathbf{G}(2\mathbf{V}^* + \boldsymbol{\mu}^*) \geq 0, \forall \mathbf{V} \in \Omega_{\mathbf{V}} \quad (7)$$

$$(\mathbf{I} - \mathbf{I}^*)^T (\boldsymbol{\eta}^* - \boldsymbol{\mu}^*) \geq 0, \forall \mathbf{I} \in \Omega_{\mathbf{I}} \quad (8)$$

$$\mathbf{I}^* = \mathbf{G}\mathbf{V}^* + \mathbf{I}_{\mathbf{L}} \quad (9)$$

where  $\boldsymbol{\eta}^* = [\eta_1^*, \eta_2^*, \dots, \eta_m^*]^T \in \mathbb{R}^n$  with

$$\eta_i^* = \nabla C_{\text{conv}_i}(I_i^*) = 2a_i I_i^* + b_i \text{sgn}(I_i^*), i \in \mathcal{V}_E. \quad (10)$$

*Proof:* Considering the fact that  $\mathbf{G} = \mathbf{G}^T$ , the proof of Lemma 1 can be directly obtained based on the theoretical results in [39, Lemma 2] and thus is omitted here.

*Remark 1:* Assumption 1 ensures the existence of a feasible solution for the convex optimization problem (4). For a well-designed dc microgrid, this assumption can be always satisfied.

### B. Equivalent Optimality Condition

To aid the development of the distributed optimal control law in Section IV, an equivalent necessary and sufficient condition for the optimal solution to the optimization problem (4) is derived in this section. Before proceeding, the project operator  $\mathbf{P}_{\mathcal{X}}(\bullet) : \mathbb{R}^m \rightarrow \mathbb{R}^m$  [40] is introduced to transform the original inequality conditions (7) and (8) to equivalent equality conditions. For a vector  $\mathbf{z} \in \mathbb{R}^m$ , its projection on a nonempty closed convex set  $\mathcal{X} \subseteq \mathbb{R}^m$  is defined as

$$\mathbf{P}_{\mathcal{X}}(\mathbf{z}) = \arg \min_{\mathbf{y} \in \mathcal{X}} \|\mathbf{z} - \mathbf{y}\|. \quad (11)$$

Moreover, the properties of the project operator  $\mathbf{P}_{\mathcal{X}}$  are stated in the following lemma.

*Lemma 2* [40]: Assume that  $\mathcal{X} \subseteq \mathbb{R}^m$  is a closed convex set. Then, one has

$$(\mathbf{y} - \mathbf{P}_{\mathcal{X}}(\mathbf{z}))^T (\mathbf{P}_{\mathcal{X}}(\mathbf{z}) - \mathbf{z}) \geq 0, \forall \mathbf{z} \in \mathbb{R}^m, \mathbf{y} \in \mathcal{X}. \quad (12)$$

Now, an equivalent necessary and sufficient condition for the optimal solution to the optimization problem (4), which can be further used for control designs, is stated in the following theorem.

*Theorem 1:* With Assumption 1,  $(\mathbf{V}^*, \mathbf{I}^*)$  is an optimal solution to problem (4) if and only if there exist  $\boldsymbol{\mu}^* \in \mathbb{R}^n$  such that

$$\mathbf{V}^* = \mathbf{P}_{\Omega_{\mathbf{V}}}(\mathbf{V}^* - \mathbf{G}(2\mathbf{V}^* + \boldsymbol{\mu}^*)) \quad (13)$$

$$\mathbf{I}^* = \mathbf{P}_{\Omega_{\mathbf{I}}}(\mathbf{I}^* - \boldsymbol{\eta}^* + \boldsymbol{\mu}^*) \quad (14)$$

$$\mathbf{I}^* = \mathbf{G}\mathbf{V}^* + \mathbf{I}_{\mathbf{L}}. \quad (15)$$

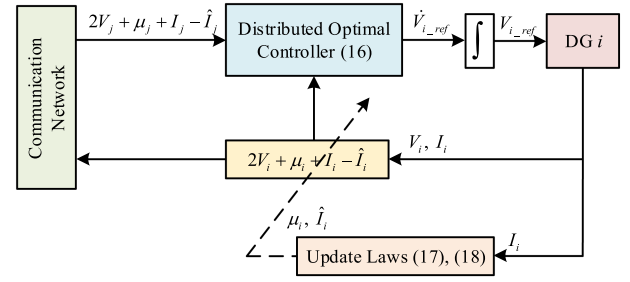


Fig. 2. Diagram of the proposed control algorithm for DG  $i$ .

*Proof:* See Appendix A.

## IV. DISTRIBUTED OPTIMAL CONTROL METHODOLOGY FOR DC MICROGRIDS

### A. Distributed Optimal Controller

To solve the optimization problem (4), a distributed optimal control algorithm is introduced in this section to drive the dc microgrid to the optimal operation point in real time by dynamically updating voltage reference. Inspired by [39], the control algorithm for DG  $i$  is designed as

$$\dot{V}_{i\_ref} = \alpha \left[ \mathbf{P}_{\Omega_{V_i}} \left( V_i - \sum_{j=1}^n g_{ij} \left( (2V_i + \mu_i + I_i - \hat{I}_i) - (2V_j + \mu_j + I_j - \hat{I}_j) \right) - V_i \right) \right] \quad (16)$$

$$\dot{\hat{I}}_i = \alpha \left[ \mathbf{P}_{\Omega_{I_i}} (I_i - \eta_i + \mu_i) - \hat{I}_i \right] \quad (17)$$

$$\dot{\mu}_i = \frac{\alpha}{2} (I_i - \hat{I}_i) \quad (18)$$

where  $\Omega_{V_i} = \{V_i \in \mathbb{R} | \underline{V}_i \leq V_i \leq \bar{V}_i\}$ ,  $\Omega_{I_i} = \{I_i \in \mathbb{R} | \underline{I}_i \leq I_i \leq \bar{I}_i\}$ ,  $\alpha \in \mathbb{R}^+$  is a user-defined constant control gain,  $\hat{I}_i \in \mathbb{R}$  is an internal current control signal of DG  $i$ ,  $\eta_i = \nabla C_{\text{conv}_i}(\hat{I}_i)$ , and  $\mu_i \in \mathbb{R}$  is the integral of the error between the internal current control signal and the real output current.  $V_{i\_ref} \in \mathbb{R}$  is the voltage reference of the bus  $i$ , which will be further realized by each DG's inner control loop.

Note that in microgrids, the bus voltages and output currents are strictly governed by (2). Strictly speaking, only the bus voltages can be independently controlled for converters, whose constraints in (4) can be ensured through the project operator as designed in (16). However, the constraints on the output currents cannot be guaranteed directly through the project operator due to the relationship between bus voltages and output currents. Hence, an internal current control signal  $\hat{I}_i$  is introduced to facilitate the regulation of DGs' output currents to ensure their steady-state values satisfy (4).

### B. Control Implementation

The control diagram is given in Fig. 2. It should be noted that the proposed control algorithm (16)–(18) is distributed in the sense that each DG's local controller only requires its local information and the information from its neighbors through the communication network, as shown in Fig. 1. Moreover, for each

DG, only the lumped variable  $2V_i + \mu_i + I_i - \hat{I}_i$  is required to be transmitted to its neighbors. The exchanged information is thus limited.

## V. MAIN RESULTS

In this section, the stability and convergence of the dc microgrid under the proposed distributed optimal controller are analyzed through the Lyapunov synthesis. Moreover, individual bus voltage regulation is presented.

### A. Stability and Convergence Analysis

By virtue of modern power electronic devices, the bus voltage  $V_i$  can track its reference  $V_{i\_ref}$  generated by the designed controller quickly. Hence, it is reasonable to assume that  $V_i = V_{i\_ref}$  in the following analyses.

To facilitate the analysis, rewriting (16)–(18) in a compact form yields

$$\dot{\mathbf{V}} = \alpha \left[ \mathbf{P}_{\Omega_{\mathbf{V}}} (\mathbf{V} - \mathbf{G}(2\mathbf{V} + \boldsymbol{\mu} + \mathbf{I} - \hat{\mathbf{I}})) - \mathbf{V} \right] \quad (19)$$

$$\dot{\hat{\mathbf{I}}} = \alpha \left[ \mathbf{P}_{\Omega_{\hat{\mathbf{I}}}} (\mathbf{I} - \boldsymbol{\eta} + \boldsymbol{\mu}) - \hat{\mathbf{I}} \right] \quad (20)$$

$$\dot{\boldsymbol{\mu}} = \frac{\alpha}{2} (\mathbf{I} - \hat{\mathbf{I}}) \quad (21)$$

where  $\hat{\mathbf{I}} = [\hat{I}_1, \hat{I}_2, \dots, \hat{I}_n]^T \in \mathbb{R}^n$ ,  $\boldsymbol{\mu} = [\mu_1, \mu_2, \dots, \mu_n]^T \in \mathbb{R}^n$ , and  $\boldsymbol{\eta} = [\eta_1, \eta_2, \dots, \eta_n]^T \in \mathbb{R}^n$ .

The stability and convergence analyses of the proposed distributed optimal controller are illustrated in the following theorem.

*Theorem 2:* Consider a dc microgrid described by (3) satisfying Assumption 1. If the distributed optimal control law is designed as (16)–(18), then the bus voltages and output currents converge to their optima asymptotically.

*Proof:* See Appendix B.

*Remark 2:* To achieve online operation loss minimization, controllers must be able to respond quickly to load changes. Such a feature is directly reflected in our control design (16)–(18), where the local bus voltage  $V_i$  and output current  $I_i$  is measured to promptly feedback any local load change to the controller without the measurement of the load current  $I_{L_i}$ . Additionally, the large-signal stability of the closed-loop system is ensured via Lyapunov synthesis, which implies that if load changes, the proposed optimal controller can respond immediately and dynamically drive the dc microgrid to the new optimal operating condition irrespective of the original operating point. Thus, the proposed optimal controller can achieve online operation loss minimization.

### B. Individual Bus Voltage Regulation

According to (16) and the assumption  $V_i = V_{i\_ref}$ , one has  $\dot{V}_i = \alpha(\tilde{P}_{\Omega_{V_i}} - V_i)$  with

$$\begin{aligned} \tilde{P}_{\Omega_{V_i}} = & \mathbf{P}_{\Omega_{V_i}} \left( V_i - \sum_{j=1}^n g_{ij} ((2V_i + \mu_i + I_i - \hat{I}_i) \right. \\ & \left. - (2V_j + \mu_j + I_j - \hat{I}_j)) \right). \end{aligned} \quad (22)$$

TABLE I  
SYSTEM PARAMETERS

Quantity	Value
Line conductance $g_{ij}$ (p.u.)	4.608
Current upper-bound $\bar{I}_i$ (p.u.)	1.0
Current lower-bound $\underline{I}_i$ (p.u.)	0.0
Voltage upper-bound $\bar{V}_i$ (p.u.)	1.05
Voltage lower-bound $\underline{V}_i$ (p.u.)	0.95
Converter loss coefficient $a_i$ ( $10^{-2}$ p.u.)	8.984, 4.644 4.644, 8.984
Converter loss coefficient $b_i$ ( $10^{-4}$ p.u.)	5.841, 5.841 5.841, 5.841
Converter loss coefficient $c_i$ ( $10^{-3}$ p.u.)	4.377, 4.364 4.375, 4.377
Filter capacitance $C_i$ ( $\mu\text{F}$ )	250, 200, 250, 250
Filter inductance $L_i$ (mH)	2.0, 2.0, 1.5, 2.0
Filter resistance $R_i$ ( $\Omega$ )	0.2, 0.1, 0.1, 0.2
Nominal bus voltage $V_{nom}$ (V)	48
Nominal power rate $P_{nom}$ (W)	1000
Switching frequency (kHz)	10

Obviously,  $\tilde{P}_{\Omega_{V_i}} \in \Omega_{V_i}$ , and subsequently, one has

$$\begin{cases} \dot{V}_i \leq 0, V_i \geq \bar{V}_i \\ \dot{V}_i \geq 0, V_i \leq \underline{V}_i \end{cases} \quad (23)$$

which indicates that the bus voltage  $V_i$  will no longer increase when it reaches its upper bound  $\bar{V}_i$  or decrease when it reaches its lower bound  $\underline{V}_i$ . Besides, for any  $V_i, i = 1, 2, \dots, n$  larger (smaller) than its upper (lower) bound, it will converge to the closed set  $\Omega_{V_i}$  and remain inside it. Consequently,  $\Omega_{\mathbf{V}}$  is an invariant set, i.e., for any  $\mathbf{V}(t_0) \in \Omega_{\mathbf{V}}$ ,  $\mathbf{V}(t) \in \Omega_{\mathbf{V}}$  holds for all  $t \geq t_0$ . Individual bus voltage regulation is thus achieved by the project operator in (16).

## VI. SIMULATION STUDIES

### A. Microgrid and Control Parameters

To evaluate the effectiveness of the designed distributed optimal controller in dc microgrids, detailed switch-level simulations are performed in MATLAB/Simulink. Each DG is modeled as a buck converter with a dc source, which is connected to the electrical network through an  $LC$  filter. The topology of the dc microgrid is demonstrated in Fig. 1. The system parameters are listed in Table I, and the converter loss coefficients are calculated according to [41]. The filter parameters are selected based on [42]. The constant control gain is selected as  $\alpha = 15$ .

### B. Case I: Proposed Optimal Control

In this case, the effectiveness of the proposed optimal controller is tested under load condition I listed in Table II.

The results are shown in Figs. 3 and 4. From Fig. 3, one can see that the bounded bus voltage regulation is ensured. Also, the output currents can be maintained in their predefined constraints successfully, as illustrated in Fig. 4. Besides, the bus voltages

TABLE II  
LOAD CONDITION I

Bus	0-1 s	1-4 s	4-7 s	7-10 s
1	0	0.4 p.u.	0.3 p.u.	0.1 p.u.
2	0	0.3 p.u.	0.1 p.u.	0
3	0	0.3 p.u.	0.2 p.u.	0.2 p.u.
4	0	0.1 p.u.	0	0

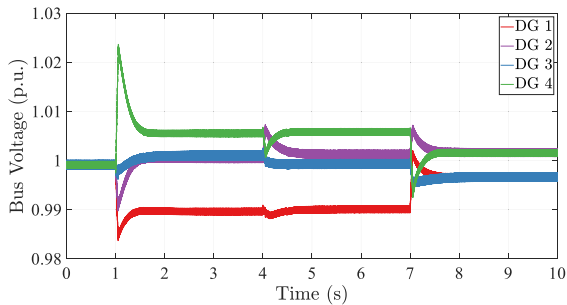


Fig. 3. Control performance of bus voltages with the proposed controller under load condition I.

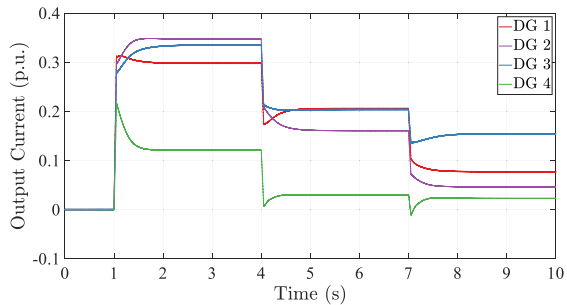


Fig. 4. Control performance of output currents with the proposed controller under load condition I.

and output currents can converge to their steady-state values in about 1 s after the occurrence of load changes. The stability of the proposed method is guaranteed.

The optimality of the proposed method is demonstrated in Table IV. The operation loss of the proposed method is directly obtained from the simulation results. The ground truth of the operation loss is obtained through the MATLAB convex optimization tool. As shown in Table IV, one can note that the relative error between the operation loss of the proposed method and that of the ground truth are almost zero. Thus, the proposed method can achieve online optimization.

### C. Case II: Comparison Studies

This case aims to test the individual bus voltage regulation capability of the proposed distributed optimal controller under the extreme load condition II listed in Table III. Comparison results with the optimal controller in [14] are also given.

The corresponding simulation results of the proposed controller are shown in Figs. 5 and 6, and those of the controller

TABLE III  
LOAD CONDITION II

Bus	0-1 s	1-4 s	4-7 s	7-10 s
1	0	0.3 p.u.	0.5 p.u.	1.8 p.u.
2	0	0.1 p.u.	0.2 p.u.	0.5 p.u.
3	0	0.1 p.u.	0.4 p.u.	0.5 p.u.
4	0	0	0.1 p.u.	0

TABLE IV  
OPERATION LOSS WITH THE PROPOSED CONTROLLER

Time	Proposed Method	Ground Truth	Relative Error	Efficiency
1-4 s	0.03940 p.u.	0.03939 p.u.	0.02539%	96.54%
4-7 s	0.02602 p.u.	0.02601 p.u.	0.03845%	95.84%
7-10 s	0.01980 p.u.	0.01978 p.u.	0.1011%	93.81%

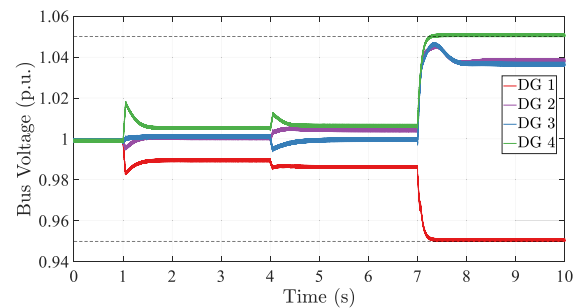


Fig. 5. Control performance of bus voltages with the proposed controller under load condition II.

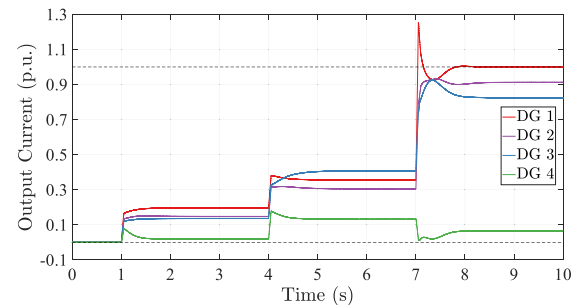


Fig. 6. Control performance of output currents with the proposed controller under load condition II.

in [14] are shown in Figs. 7 and 8. As shown in Table III, since the majority of the load requirement is concentrated on the bus of DG 1, a considerable amount of current needs to be transferred from other DGs to DG 1, which further leads to large bus voltage differences and pushes the bus voltages toward their bounds. From Fig. 5, one can see that the proposed distributed controller can achieve individual bus voltage regulation during both the transient and steady states. Under all load changes, all bus voltages are ensured to be restricted in their constraints for all time, i.e., 0.95–1.05 p.u. The convergence time is less than 1 s. For the optimal controller in [14], since only the average bus voltage is regulated, the bus voltage of DG 1 cannot be ensured

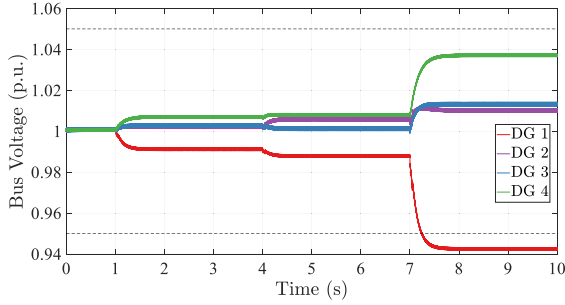


Fig. 7. Control performance of bus voltages with the controller in [14] under load condition II.

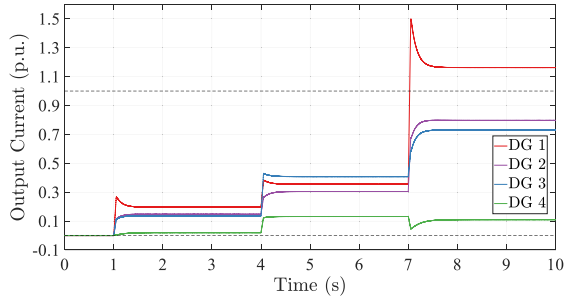


Fig. 8. Control performance of output currents with the controller in [14] under load condition II.

TABLE V  
OPERATION LOSS WITH THE PROPOSED CONTROLLER

	Proposed Method	Ground Truth	Relative Error	Efficiency
1-4 s	0.02438 p.u.	0.02439 p.u.	0.04100%	95.35%
4-7 s	0.04575 p.u.	0.04574 p.u.	0.02186%	96.33%
7-10 s	0.2496 p.u.	0.2497 p.u.	0.04005%	91.82%

TABLE VI  
OPERATION LOSS WITH THE CONTROLLER IN [14]

	Controller [14]	Ground Truth	Relative Error
1-4 s	0.02436 p.u.	0.02439 p.u.	0.1230%
4-7 s	0.04571 p.u.	0.04574 p.u.	0.06559%
7-10 s	0.2424 p.u.	0.2426 p.u.	0.08244%

to be within the secure operation range, as illustrated in Fig. 7, which may cause damage to vital and sensitive loads.

The trajectories of output currents of DGs are shown in Figs. 6 and 8 with the proposed controller and the controller in [14], respectively. From Fig. 6, one can note that the proposed controller can ensure the satisfaction of the output currents constraints in the steady state, while in the transient state, since the output currents are not directly regulated for DGs, they are not guaranteed to be within their constraints under load condition II. In Fig. 8, the trajectories of the output currents with the controller in [14] are given. One can note that the output current constraints cannot be guaranteed in both the transient and steady states since they are not considered in [14].

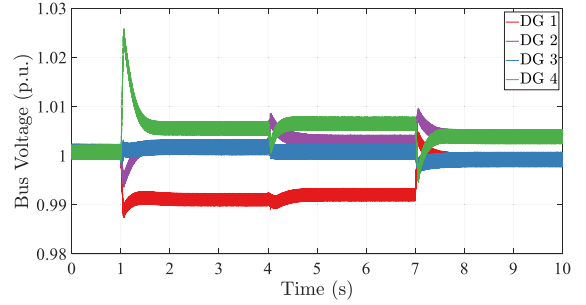


Fig. 9. Control performance of bus voltages with  $500 \mu\text{s}$  communication delay under load condition I.

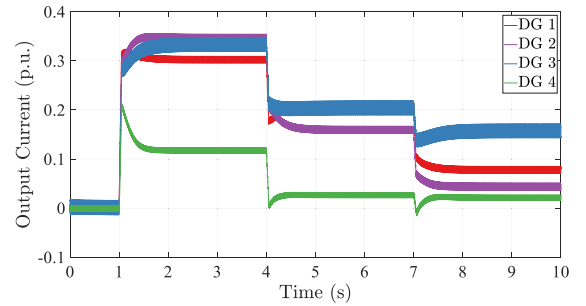


Fig. 10. Control performance of output currents with  $500 \mu\text{s}$  communication delay under load condition I.

Tables V and VI illustrate the optimality of the proposed method and the method in [14], respectively. As shown in Table V, one can note that the relative error between the operation loss of the proposed method and that of the ground truth are still very close to zero. Hence, the proposed method can achieve online optimization. In Table VI, the ground truth of the operation loss is obtained through the MATLAB convex optimization tool without bus voltage and output current constraints. By comparing Tables V and VI, one can note that the operation loss of the controller in [14] is lower than that of the proposed controller from 7 to 10 s. This is because the constraints of bus voltages and output currents are not considered for the controller in [14]. However, this optimal condition cannot be realized since the output current of DG 1 exceeds its maximum capacity.

#### D. Case III: Communication Delay

In this case, the proposed distributed optimal controller is tested with constant communication delays. The dc microgrid is subjected to load condition I, as summarized in Table II.

The control performance of the proposed optimal controller with  $500 \mu\text{s}$  communication delay is demonstrated in Figs. 9 and 10, which is similar to the one shown in Figs. 3 and 4. It is evident that the  $500 \mu\text{s}$  communication delay does not have a significant impact on the performance of the proposed controller. Subsequently, as shown in Figs. 11 and 12, a  $1500 \mu\text{s}$  communication delay is added to the communication network. In this case, the controller can still guarantee the stability of

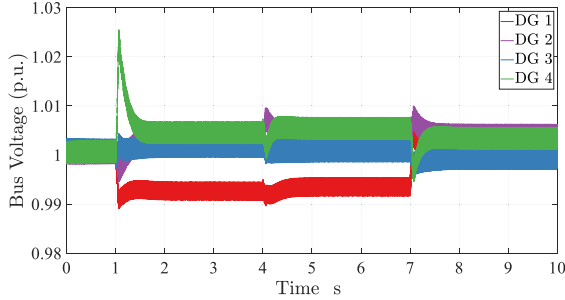


Fig. 11. Control performance of bus voltages with 1500  $\mu\text{s}$  communication delay under load condition I.

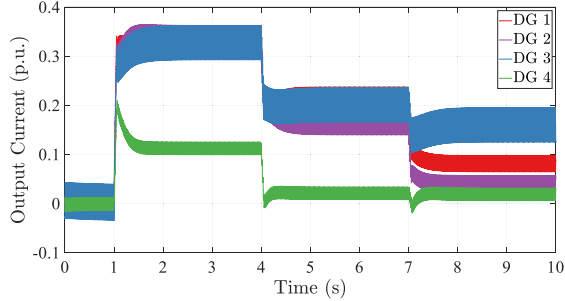


Fig. 12. Control performance of output currents with 1500  $\mu\text{s}$  communication delay under load condition I.

the system with oscillations. Based on the aforementioned studies, it can be seen that the proposed controller can withstand 1500  $\mu\text{s}$  communication delay or less.

## VII. CONCLUSION

In this article, a distributed optimal control algorithm is developed to minimize the operation loss of dc microgrids. An equivalent optimality condition is derived from the formulated optimization problem, based on which a distributed controller is designed to realize the optimization objective in real time. In addition, each individual bus voltage is regulated to avoid being dangerously high or low. The stability and convergence of the proposed algorithm are analyzed through Lyapunov synthesis. The bus voltages and output currents are proved to converge to their optima asymptotically. Finally, the effectiveness of the developed control algorithm is illustrated by detailed switch-level dc microgrid simulations.

In this article, the communication topology is considered to be identical to the electrical network since such a topology can achieve the optimal control objectives with limited information shared among DGs. In the future, the distributed optimal control design with general communication networks will be investigated.

### APPENDIX A: PROOF OF THEOREM 1

First, the equivalence between (7) and (13) is proved. Assume that (13) holds. With the help of Lemma 2, for any  $\mathbf{V} \in \Omega_{\mathbf{V}}$ , one

has

$$\begin{aligned} & (\mathbf{V} - \mathbf{V}^*)^T \mathbf{G}(2\mathbf{V}^* + \boldsymbol{\mu}^*) \\ &= (\mathbf{V} - \mathbf{P}_{\Omega_{\mathbf{V}}}(\mathbf{V}^* - \mathbf{G}(2\mathbf{V}^* + \boldsymbol{\mu}^*)))^T \\ & \times (\mathbf{P}_{\Omega_{\mathbf{V}}}(\mathbf{V}^* - \mathbf{G}(2\mathbf{V}^* + \boldsymbol{\mu}^*)) - \mathbf{V}^* + \mathbf{G}(2\mathbf{V}^* + \boldsymbol{\mu}^*)) \geq 0. \end{aligned} \quad (24)$$

For the converse, for an optimal solution  $\mathbf{V}^*$ , it satisfies  $\mathbf{V}^* \in \Omega_{\mathbf{V}}$ . Recalling Lemma 2 yields

$$\begin{aligned} & (\mathbf{V}^* - \mathbf{P}_{\Omega_{\mathbf{V}}}(\mathbf{V}^* - \mathbf{G}(2\mathbf{V}^* + \boldsymbol{\mu}^*)))^T \\ & \times (\mathbf{P}_{\Omega_{\mathbf{V}}}(\mathbf{V}^* - \mathbf{G}(2\mathbf{V}^* + \boldsymbol{\mu}^*)) - \mathbf{V}^* + \mathbf{G}(2\mathbf{V}^* + \boldsymbol{\mu}^*)) \geq 0. \end{aligned} \quad (25)$$

If (7) holds, then

$$\begin{aligned} & \|\mathbf{P}_{\Omega_{\mathbf{V}}}(\mathbf{V}^* - \mathbf{G}(2\mathbf{V}^* + \boldsymbol{\mu}^*)) - \mathbf{V}^*\|^2 \\ & \leq (\mathbf{V}^* - \mathbf{P}_{\Omega_{\mathbf{V}}}(\mathbf{V}^* - \mathbf{G}(2\mathbf{V}^* + \boldsymbol{\mu}^*)))^T \mathbf{G}(2\mathbf{V}^* + \boldsymbol{\mu}^*) \leq 0. \end{aligned} \quad (26)$$

Thus,  $\mathbf{V}^* = \mathbf{P}_{\Omega_{\mathbf{V}}}(\mathbf{V}^* - \mathbf{G}(2\mathbf{V}^* + \boldsymbol{\mu}^*))$  holds. Equations (7) and (13) are equivalent.

Next, the equivalence between (8) and (14) is illustrated. Assume that (14) holds. With the help of (12), one has

$$\begin{aligned} & (\mathbf{I} - \mathbf{I}^*)^T (\boldsymbol{\eta}^* - \boldsymbol{\mu}^*) = (\mathbf{I} - \mathbf{P}_{\Omega_{\mathbf{I}}}(\mathbf{I}^* - \boldsymbol{\eta}^* + \boldsymbol{\mu}^*))^T \\ & \times (\mathbf{P}_{\Omega_{\mathbf{I}}}(\mathbf{I}^* - \boldsymbol{\eta}^* + \boldsymbol{\mu}^*) - \mathbf{I}^* + \boldsymbol{\eta}^* - \boldsymbol{\mu}^*) \geq 0, \forall \mathbf{I} \in \Omega_{\mathbf{I}}. \end{aligned} \quad (27)$$

For the converse, first, one has  $\mathbf{I}^* \in \Omega_{\mathbf{I}}$ . According to (12), the following inequality holds:

$$\begin{aligned} & (\mathbf{I}^* - \mathbf{P}_{\Omega_{\mathbf{I}}}(\mathbf{I}^* - \boldsymbol{\eta}^* + \boldsymbol{\mu}^*))^T \\ & \times (\mathbf{P}_{\Omega_{\mathbf{I}}}(\mathbf{I}^* - \boldsymbol{\eta}^* + \boldsymbol{\mu}^*) - \mathbf{I}^* + \boldsymbol{\eta}^* - \boldsymbol{\mu}^*) \geq 0. \end{aligned} \quad (28)$$

If (8) is satisfied, then one has

$$\begin{aligned} & \|\mathbf{P}_{\Omega_{\mathbf{I}}}(\mathbf{I}^* - \boldsymbol{\eta}^* + \boldsymbol{\mu}^*) - \mathbf{I}^*\|^2 \\ & \leq (\mathbf{I}^* - \mathbf{P}_{\Omega_{\mathbf{I}}}(\mathbf{I}^* - \boldsymbol{\eta}^* + \boldsymbol{\mu}^*))^T (\boldsymbol{\eta}^* - \boldsymbol{\mu}^*) \leq 0. \end{aligned} \quad (29)$$

Thus,  $\mathbf{I}^* = \mathbf{P}_{\Omega_{\mathbf{I}}}(\mathbf{I}^* - \boldsymbol{\eta}^* + \boldsymbol{\mu}^*)$ . Equations (8) and (14) are equivalent.

Furthermore, note that (9) and (15) are identical. Hence, (13)–(15) are the equivalent necessary and have sufficient condition for the optimal solution to the optimization problem (4). Thus, Theorem 1 holds.

### APPENDIX B: PROOF OF THEOREM 2

Define  $\Delta_{\mathbf{V}} = \mathbf{G}(2\mathbf{V} + \boldsymbol{\mu} + \mathbf{I} - \hat{\mathbf{I}})$  and  $\Delta_{\mathbf{I}} = \boldsymbol{\eta} - \boldsymbol{\mu} - \mathbf{I} + \hat{\mathbf{I}}$  for simplicity. Then, (19) and (20) can be rewritten as

$$\dot{\mathbf{V}} = \alpha[\mathbf{P}_{\Omega_{\mathbf{V}}}(\mathbf{V} - \Delta_{\mathbf{V}}) - \mathbf{V}] \quad (30)$$

$$\dot{\hat{\mathbf{I}}} = \alpha[\mathbf{P}_{\Omega_{\mathbf{I}}}(\hat{\mathbf{I}} - \Delta_{\mathbf{I}}) - \hat{\mathbf{I}}]. \quad (31)$$

The convergence and stability of the proposed controller are proved by the Lyapunov theory. Consider the following Lyapunov candidate function [39]:

$$\begin{aligned}
W = & \frac{1}{\alpha} \left\{ C(\hat{\mathbf{I}}, \mathbf{V}) - C(\mathbf{I}^*, \mathbf{V}^*) - (2\mathbf{G}\mathbf{V}^*)^T (\mathbf{V} - \mathbf{V}^*) \right. \\
& - (\boldsymbol{\eta}^*)^T (\hat{\mathbf{I}} - \mathbf{I}^*) + \frac{1}{2} \|\boldsymbol{\mu} - \boldsymbol{\mu}^* + \mathbf{I} - \hat{\mathbf{I}}\|^2 + \frac{1}{2} \|\mathbf{V} - \mathbf{V}^*\|^2 \\
& \left. + \frac{1}{2} \|\hat{\mathbf{I}} - \mathbf{I}^*\|^2 + \frac{1}{2} \|\boldsymbol{\mu} - \boldsymbol{\mu}^*\|^2 \right\}. \quad (32)
\end{aligned}$$

Note that  $W$  is a function of  $\mathbf{V}$ ,  $\hat{\mathbf{I}}$ ,  $\boldsymbol{\mu}$ . Taking the time derivative of  $W$  yields

$$\dot{W} = \frac{\partial W}{\partial \mathbf{V}} \dot{\mathbf{V}} + \frac{\partial W}{\partial \hat{\mathbf{I}}} \dot{\hat{\mathbf{I}}} + \frac{\partial W}{\partial \boldsymbol{\mu}} \dot{\boldsymbol{\mu}}. \quad (33)$$

Substituting (30) into the first term of  $\dot{W}$  yields

$$\begin{aligned}
\frac{\partial W}{\partial \mathbf{V}} \dot{\mathbf{V}} &= \left[ \mathbf{G} (2\mathbf{V} - 2\mathbf{V}^* + \boldsymbol{\mu} - \boldsymbol{\mu}^* + \mathbf{I} - \hat{\mathbf{I}}) + \mathbf{V} - \mathbf{V}^* \right]^T \frac{\dot{\mathbf{V}}}{\alpha} \\
&= (\boldsymbol{\Delta}_{\mathbf{V}} - \boldsymbol{\Delta}_{\mathbf{V}}^* + \mathbf{V} - \mathbf{V}^*)^T (\mathbf{P}_{\Omega_{\mathbf{V}}}(\mathbf{V} - \boldsymbol{\Delta}_{\mathbf{V}}) - \mathbf{V}) \\
&= (\boldsymbol{\Delta}_{\mathbf{V}} - \boldsymbol{\Delta}_{\mathbf{V}}^* + \mathbf{P}_{\Omega_{\mathbf{V}}}(\mathbf{V} - \boldsymbol{\Delta}_{\mathbf{V}}) - \mathbf{V}^*)^T \\
&\quad \times (\mathbf{P}_{\Omega_{\mathbf{V}}}(\mathbf{V} - \boldsymbol{\Delta}_{\mathbf{V}}) - \mathbf{V}) - \|\mathbf{V} - \mathbf{P}_{\Omega_{\mathbf{V}}}(\mathbf{V} - \boldsymbol{\Delta}_{\mathbf{V}})\|^2 \quad (34)
\end{aligned}$$

where  $\boldsymbol{\Delta}_{\mathbf{V}}^* = \mathbf{G}(2\mathbf{V}^* + \boldsymbol{\mu}^*)$ . For the first term of the last equality in (34), one has

$$\begin{aligned}
&(\boldsymbol{\Delta}_{\mathbf{V}} - \boldsymbol{\Delta}_{\mathbf{V}}^* + \mathbf{P}_{\Omega_{\mathbf{V}}}(\mathbf{V} - \boldsymbol{\Delta}_{\mathbf{V}}) - \mathbf{V}^*)^T (\mathbf{P}_{\Omega_{\mathbf{V}}}(\mathbf{V} - \boldsymbol{\Delta}_{\mathbf{V}}) - \mathbf{V}) \\
&= (\boldsymbol{\Delta}_{\mathbf{V}} - \boldsymbol{\Delta}_{\mathbf{V}}^* + \mathbf{P}_{\Omega_{\mathbf{V}}}(\mathbf{V} - \boldsymbol{\Delta}_{\mathbf{V}}) - \mathbf{V})^T (\mathbf{P}_{\Omega_{\mathbf{V}}}(\mathbf{V} - \boldsymbol{\Delta}_{\mathbf{V}}) - \mathbf{V}^*) \\
&\quad - (\boldsymbol{\Delta}_{\mathbf{V}} - \boldsymbol{\Delta}_{\mathbf{V}}^*)^T (\mathbf{V} - \mathbf{V}^*) \\
&= (\mathbf{P}_{\Omega_{\mathbf{V}}}(\mathbf{V} - \boldsymbol{\Delta}_{\mathbf{V}}) - (\mathbf{V} - \boldsymbol{\Delta}_{\mathbf{V}}))^T (\mathbf{P}_{\Omega_{\mathbf{V}}}(\mathbf{V} - \boldsymbol{\Delta}_{\mathbf{V}}) - \mathbf{V}^*) \\
&\quad - (\boldsymbol{\Delta}_{\mathbf{V}}^*)^T (\mathbf{P}_{\Omega_{\mathbf{V}}}(\mathbf{V} - \boldsymbol{\Delta}_{\mathbf{V}}) - \mathbf{V}^*) - (\boldsymbol{\Delta}_{\mathbf{V}} - \boldsymbol{\Delta}_{\mathbf{V}}^*)^T (\mathbf{V} - \mathbf{V}^*). \quad (35)
\end{aligned}$$

For the first two terms of the last equality in (35), according to Lemma 2 and (7), one has

$$(\mathbf{P}_{\Omega_{\mathbf{V}}}(\mathbf{V} - \boldsymbol{\Delta}_{\mathbf{V}}) - (\mathbf{V} - \boldsymbol{\Delta}_{\mathbf{V}}))^T (\mathbf{P}_{\Omega_{\mathbf{V}}}(\mathbf{V} - \boldsymbol{\Delta}_{\mathbf{V}}) - \mathbf{V}^*) \leq 0 \quad (36)$$

and

$$(\boldsymbol{\Delta}_{\mathbf{V}}^*)^T (\mathbf{P}_{\Omega_{\mathbf{V}}}(\mathbf{V} - \boldsymbol{\Delta}_{\mathbf{V}}) - \mathbf{V}^*) \geq 0. \quad (37)$$

Thereafter, combining (35)–(37) gives

$$\begin{aligned}
&(\boldsymbol{\Delta}_{\mathbf{V}} - \boldsymbol{\Delta}_{\mathbf{V}}^* + \mathbf{P}_{\Omega_{\mathbf{V}}}(\mathbf{V} - \boldsymbol{\Delta}_{\mathbf{V}}) - \mathbf{V}^*)^T (\mathbf{P}_{\Omega_{\mathbf{V}}}(\mathbf{V} - \boldsymbol{\Delta}_{\mathbf{V}}) - \mathbf{V}) \\
&\leq -(\boldsymbol{\Delta}_{\mathbf{V}} - \boldsymbol{\Delta}_{\mathbf{V}}^*)^T (\mathbf{V} - \mathbf{V}^*). \quad (38)
\end{aligned}$$

Substituting (38) into (34) yields

$$\begin{aligned}
\frac{\partial W}{\partial \mathbf{V}} \dot{\mathbf{V}} &\leq -\|\mathbf{V} - \mathbf{P}_{\Omega_{\mathbf{V}}}(\mathbf{V} - \boldsymbol{\Delta}_{\mathbf{V}})\|^2 \\
&\quad - (\boldsymbol{\Delta}_{\mathbf{V}} - \boldsymbol{\Delta}_{\mathbf{V}}^*)^T (\mathbf{V} - \mathbf{V}^*). \quad (39)
\end{aligned}$$

Next, substituting (31) into the second term of  $\dot{W}$  yields

$$\begin{aligned}
\frac{\partial W}{\partial \hat{\mathbf{I}}} \dot{\hat{\mathbf{I}}} &= \left[ \boldsymbol{\eta} - \boldsymbol{\eta}^* - (\boldsymbol{\mu} - \boldsymbol{\mu}^* + \mathbf{I} - \hat{\mathbf{I}}) + \hat{\mathbf{I}} - \mathbf{I}^* \right]^T \frac{\dot{\hat{\mathbf{I}}}}{\alpha} \\
&= (\boldsymbol{\Delta}_{\mathbf{I}} - \boldsymbol{\Delta}_{\mathbf{I}}^* + \hat{\mathbf{I}} - \mathbf{I}^*)^T (\mathbf{P}_{\Omega_{\mathbf{I}}}(\hat{\mathbf{I}} - \boldsymbol{\Delta}_{\mathbf{I}}) - \hat{\mathbf{I}})
\end{aligned}$$

$$\begin{aligned}
&= (\boldsymbol{\Delta}_{\mathbf{I}} - \boldsymbol{\Delta}_{\mathbf{I}}^* + \mathbf{P}_{\Omega_{\mathbf{I}}}(\hat{\mathbf{I}} - \boldsymbol{\Delta}_{\mathbf{I}}) - \mathbf{I}^*)^T \\
&\quad \times (\mathbf{P}_{\Omega_{\mathbf{I}}}(\hat{\mathbf{I}} - \boldsymbol{\Delta}_{\mathbf{I}}) - \hat{\mathbf{I}}) - \left\| \hat{\mathbf{I}} - \mathbf{P}_{\Omega_{\mathbf{I}}}(\hat{\mathbf{I}} - \boldsymbol{\Delta}_{\mathbf{I}}) \right\|^2 \quad (40)
\end{aligned}$$

where  $\boldsymbol{\Delta}_{\mathbf{I}}^* = \boldsymbol{\eta}^* - \boldsymbol{\mu}^*$ . Again, for the first term of the last equality in (40), one has

$$\begin{aligned}
&(\boldsymbol{\Delta}_{\mathbf{I}} - \boldsymbol{\Delta}_{\mathbf{I}}^* + \mathbf{P}_{\Omega_{\mathbf{I}}}(\hat{\mathbf{I}} - \boldsymbol{\Delta}_{\mathbf{I}}) - \mathbf{I}^*)^T (\mathbf{P}_{\Omega_{\mathbf{I}}}(\hat{\mathbf{I}} - \boldsymbol{\Delta}_{\mathbf{I}}) - \hat{\mathbf{I}}) \\
&= (\boldsymbol{\Delta}_{\mathbf{I}} - \boldsymbol{\Delta}_{\mathbf{I}}^* + \mathbf{P}_{\Omega_{\mathbf{I}}}(\hat{\mathbf{I}} - \boldsymbol{\Delta}_{\mathbf{I}}) - \hat{\mathbf{I}})^T (\mathbf{P}_{\Omega_{\mathbf{I}}}(\hat{\mathbf{I}} - \boldsymbol{\Delta}_{\mathbf{I}}) - \mathbf{I}^*) \\
&\quad - (\boldsymbol{\Delta}_{\mathbf{I}} - \boldsymbol{\Delta}_{\mathbf{I}}^*)^T (\hat{\mathbf{I}} - \mathbf{I}^*) \\
&= (\mathbf{P}_{\Omega_{\mathbf{I}}}(\hat{\mathbf{I}} - \boldsymbol{\Delta}_{\mathbf{I}}) - (\hat{\mathbf{I}} - \boldsymbol{\Delta}_{\mathbf{I}}))^T (\mathbf{P}_{\Omega_{\mathbf{I}}}(\hat{\mathbf{I}} - \boldsymbol{\Delta}_{\mathbf{I}}) - \mathbf{I}^*) \\
&\quad - (\boldsymbol{\Delta}_{\mathbf{I}}^*)^T (\mathbf{P}_{\Omega_{\mathbf{I}}}(\hat{\mathbf{I}} - \boldsymbol{\Delta}_{\mathbf{I}}) - \mathbf{I}^*) - (\boldsymbol{\Delta}_{\mathbf{I}} - \boldsymbol{\Delta}_{\mathbf{I}}^*)^T (\hat{\mathbf{I}} - \mathbf{I}^*). \quad (41)
\end{aligned}$$

According to Lemma 2 and (8), one has

$$(\mathbf{P}_{\Omega_{\mathbf{I}}}(\hat{\mathbf{I}} - \boldsymbol{\Delta}_{\mathbf{I}}) - (\hat{\mathbf{I}} - \boldsymbol{\Delta}_{\mathbf{I}}))^T (\mathbf{P}_{\Omega_{\mathbf{I}}}(\hat{\mathbf{I}} - \boldsymbol{\Delta}_{\mathbf{I}}) - \mathbf{I}^*) \leq 0 \quad (42)$$

and

$$(\boldsymbol{\Delta}_{\mathbf{I}}^*)^T (\mathbf{P}_{\Omega_{\mathbf{I}}}(\hat{\mathbf{I}} - \boldsymbol{\Delta}_{\mathbf{I}}) - \mathbf{I}^*) \geq 0. \quad (43)$$

Next, combining (41)–(43) gives

$$\begin{aligned}
&(\boldsymbol{\Delta}_{\mathbf{I}} - \boldsymbol{\Delta}_{\mathbf{I}}^* + \mathbf{P}_{\Omega_{\mathbf{I}}}(\hat{\mathbf{I}} - \boldsymbol{\Delta}_{\mathbf{I}}) - \mathbf{I}^*)^T (\mathbf{P}_{\Omega_{\mathbf{I}}}(\hat{\mathbf{I}} - \boldsymbol{\Delta}_{\mathbf{I}}) - \hat{\mathbf{I}}) \\
&\leq -(\boldsymbol{\Delta}_{\mathbf{I}} - \boldsymbol{\Delta}_{\mathbf{I}}^*)^T (\hat{\mathbf{I}} - \mathbf{I}^*). \quad (44)
\end{aligned}$$

Hence, substituting (44) into (40) yields

$$\frac{\partial W}{\partial \hat{\mathbf{I}}} \dot{\hat{\mathbf{I}}} = -\left\| \hat{\mathbf{I}} - \mathbf{P}_{\Omega_{\mathbf{I}}}(\hat{\mathbf{I}} - \boldsymbol{\Delta}_{\mathbf{I}}) \right\|^2 - (\boldsymbol{\Delta}_{\mathbf{I}} - \boldsymbol{\Delta}_{\mathbf{I}}^*)^T (\hat{\mathbf{I}} - \mathbf{I}^*). \quad (45)$$

Recalling the definition of  $\boldsymbol{\Delta}_{\mathbf{V}}$ ,  $\boldsymbol{\Delta}_{\mathbf{V}}^*$ ,  $\boldsymbol{\Delta}_{\mathbf{I}}$ , and  $\boldsymbol{\Delta}_{\mathbf{I}}^*$  yields

$$\begin{aligned}
&(\boldsymbol{\Delta}_{\mathbf{V}} - \boldsymbol{\Delta}_{\mathbf{V}}^*)^T (\mathbf{V} - \mathbf{V}^*) + (\boldsymbol{\Delta}_{\mathbf{I}} - \boldsymbol{\Delta}_{\mathbf{I}}^*)^T (\hat{\mathbf{I}} - \mathbf{I}^*) \\
&= (\boldsymbol{\mu} - \boldsymbol{\mu}^* + \mathbf{I} - \hat{\mathbf{I}})^T (\mathbf{G}(\mathbf{V} - \mathbf{V}^*) - \hat{\mathbf{I}} + \mathbf{I}^*) \\
&\quad + 2(\mathbf{V} - \mathbf{V}^*)^T \mathbf{G}(\mathbf{V} - \mathbf{V}^*) + (\boldsymbol{\eta} - \boldsymbol{\eta}^*)^T (\hat{\mathbf{I}} - \mathbf{I}^*). \quad (46)
\end{aligned}$$

Due to the convexity of  $C(\mathbf{V}, \mathbf{I})$ , the last two terms in (46) satisfy

$$2(\mathbf{V} - \mathbf{V}^*)^T \mathbf{G}(\mathbf{V} - \mathbf{V}^*) + (\boldsymbol{\eta} - \boldsymbol{\eta}^*)^T (\hat{\mathbf{I}} - \mathbf{I}^*) \geq 0. \quad (47)$$

Then, (46) becomes

$$\begin{aligned}
&(\boldsymbol{\Delta}_{\mathbf{V}} - \boldsymbol{\Delta}_{\mathbf{V}}^*)^T (\mathbf{V} - \mathbf{V}^*) + (\boldsymbol{\Delta}_{\mathbf{I}} - \boldsymbol{\Delta}_{\mathbf{I}}^*)^T (\hat{\mathbf{I}} - \mathbf{I}^*) \\
&\geq (\boldsymbol{\mu} - \boldsymbol{\mu}^* + \mathbf{I} - \hat{\mathbf{I}})^T (\mathbf{G}(\mathbf{V} - \mathbf{V}^*) - \hat{\mathbf{I}} + \mathbf{I}^*). \quad (48)
\end{aligned}$$

With the help of the dc microgrid model (3), one has

$$\mathbf{G}(\mathbf{V} - \mathbf{V}^*) = \mathbf{I} - \mathbf{I}_{\mathbf{L}} - \mathbf{G}\mathbf{V}^* = \mathbf{I} - \mathbf{I}^*. \quad (49)$$

Hence, (48) becomes

$$\begin{aligned}
&(\boldsymbol{\Delta}_{\mathbf{V}} - \boldsymbol{\Delta}_{\mathbf{V}}^*)^T (\mathbf{V} - \mathbf{V}^*) + (\boldsymbol{\Delta}_{\mathbf{I}} - \boldsymbol{\Delta}_{\mathbf{I}}^*)^T (\hat{\mathbf{I}} - \mathbf{I}^*) \\
&\geq (\boldsymbol{\mu} - \boldsymbol{\mu}^* + \mathbf{I} - \hat{\mathbf{I}})^T (\mathbf{I} - \hat{\mathbf{I}}) \\
&\geq (\boldsymbol{\mu} - \boldsymbol{\mu}^*)^T (\mathbf{I} - \hat{\mathbf{I}}) + \left\| \mathbf{I} - \hat{\mathbf{I}} \right\|^2. \quad (50)
\end{aligned}$$

Thereafter, combining (39), (45), and (50) yields

$$\begin{aligned} \frac{\partial W}{\partial \mathbf{V}} \frac{\dot{\mathbf{V}}}{\alpha} + \frac{\partial W}{\partial \hat{\mathbf{I}}} \frac{\dot{\hat{\mathbf{I}}}}{\alpha} &\leq -\|\mathbf{V} - \mathbf{P}_{\Omega_{\mathbf{V}}}(\mathbf{V} - \Delta_{\mathbf{V}})\|^2 \\ &- \left\| \hat{\mathbf{I}} - \mathbf{P}_{\Omega_{\mathbf{I}}}(\hat{\mathbf{I}} - \Delta_{\mathbf{I}}) \right\|^2 - (\boldsymbol{\mu} - \boldsymbol{\mu}^*)^T (\mathbf{I} - \hat{\mathbf{I}}) - \left\| \mathbf{I} - \hat{\mathbf{I}} \right\|^2. \end{aligned} \quad (51)$$

Now, substituting (21) into the last term of (33) yields

$$\frac{\partial W}{\partial \boldsymbol{\mu}} \frac{\dot{\boldsymbol{\mu}}}{\alpha} = (\boldsymbol{\mu} - \boldsymbol{\mu}^*)^T (\mathbf{I} - \hat{\mathbf{I}}) + \frac{1}{2} \left\| \mathbf{I} - \hat{\mathbf{I}} \right\|^2. \quad (52)$$

Finally, by combining (33), (51), and (52), the time derivative of  $W$  becomes

$$\begin{aligned} \dot{W} &\leq -\frac{1}{2} \left\| \mathbf{I} - \hat{\mathbf{I}} \right\|^2 - \|\mathbf{V} - \mathbf{P}_{\Omega_{\mathbf{V}}}(\mathbf{V} - \Delta_{\mathbf{V}})\|^2 \\ &- \left\| \hat{\mathbf{I}} - \mathbf{P}_{\Omega_{\mathbf{I}}}(\hat{\mathbf{I}} - \Delta_{\mathbf{I}}) \right\|^2 \leq 0. \end{aligned} \quad (53)$$

Hence, according to the Lyapunov theory,  $\mathbf{V}$ ,  $\hat{\mathbf{I}}$ , and  $\boldsymbol{\mu}$  are all bounded. Furthermore, with the help of (3), the boundedness of  $\mathbf{V}$  and  $\mathbf{I}_{\mathbf{L}}$  yields that  $\mathbf{I}$  is also bounded. Moreover, according to the LaSalle invariance principle [43], one has  $\dot{W} = 0$ . Then, the following results can be obtained as

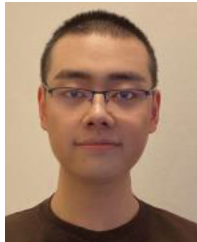
$$\begin{cases} \lim_{t \rightarrow \infty} (\mathbf{V} - \mathbf{P}_{\Omega_{\mathbf{V}}}(\mathbf{V} - \Delta_{\mathbf{V}})) = 0 \\ \lim_{t \rightarrow \infty} (\hat{\mathbf{I}} - \mathbf{P}_{\Omega_{\mathbf{I}}}(\hat{\mathbf{I}} - \Delta_{\mathbf{I}})) = 0 \\ \lim_{t \rightarrow \infty} (\mathbf{I} - \hat{\mathbf{I}}) = 0. \end{cases} \quad (54)$$

Additionally, (3) always holds for the bus voltage  $\mathbf{V}$  and the output current  $\mathbf{I}$ . Thus, all conditions in Theorem 1 are satisfied.  $\mathbf{V}$  and  $\mathbf{I}$  will finally converge to an optimal solution to the optimization problem (4).

## REFERENCES

- [1] P. Mathew, S. Madichetty, and S. Mishra, "A multilevel distributed hybrid control scheme for islanded DC microgrids," *IEEE Syst. J.*, vol. 13, no. 4, pp. 4200–4207, Dec. 2019.
- [2] Q. Xu, Y. Xu, C. Zhang, and P. Wang, "A robust droop-based autonomous controller for decentralized power sharing in DC microgrid considering large signal stability," *IEEE Trans. Ind. Informat.*, vol. 16, no. 3, pp. 1483–1494, Mar. 2020.
- [3] T. Dragičević, "Dynamic stabilization of DC microgrids with predictive control of point-of-load converters," *IEEE Trans. Power Electron.*, vol. 33, no. 12, pp. 10872–10884, Dec. 2018.
- [4] A. Afshari, M. Karrari, H. R. Baghaee, and G. B. Gharehpetian, "Resilient cooperative control of AC microgrids considering relative state-dependent noises and communication time-delays," *IET Renew. Power Gener.*, vol. 14, no. 8, pp. 1321–1331, Jun. 2020.
- [5] M. Raeispour, H. Atrianfar, H. R. Baghaee, and G. B. Gharehpetian, "Distributed LMI-based control of heterogeneous microgrids considering fixed time-delays and switching topologies," *IET Renew. Power Gener.*, vol. 14, no. 12, pp. 2068–2078, Sep. 2020.
- [6] A. Afshari, M. Karrari, H. R. Baghaee, G. Gharehpetian, and S. Karrari, "Cooperative fault-tolerant control of microgrids under switching communication topology," *IEEE Trans. Smart Grid*, vol. 11, no. 3, pp. 1866–1879, May 2020.
- [7] R. Babazadeh-Dizaji and M. Hamzeh, "Distributed hierarchical control for optimal power dispatch in multiple DC microgrids," *IEEE Syst. J.*, vol. 14, no. 1, pp. 1015–1023, Mar. 2020.
- [8] D. Xu, W. Zhang, B. Jiang, P. Shi, and S. Wang, "Directed-graph-observer-based model-free cooperative sliding mode control for distributed energy storage systems in DC microgrid," *IEEE Trans. Ind. Informat.*, vol. 16, no. 2, pp. 1224–1235, Feb. 2020.
- [9] A. Afshari, M. Karrari, H. R. Baghaee, and G. Gharehpetian, "Resilient synchronization of voltage/frequency in AC microgrids under deception attacks," *IEEE Syst. J.*, to be published, doi: [10.1109/JSYST.2020.2992309](https://doi.org/10.1109/JSYST.2020.2992309).
- [10] J. Lai, X. Lu, X. Yu, and A. Monti, "Cluster-oriented distributed cooperative control for multiple AC microgrids," *IEEE Trans. Ind. Informat.*, vol. 15, no. 11, pp. 5906–5918, Nov. 2019.
- [11] M. Raeispour, H. Atrianfar, H. R. Baghaee, and G. Gharehpetian, "Resilient H- $\infty$  consensus-based control of autonomous AC microgrids with uncertain time-delayed communications," *IEEE Trans. Smart Grid*, vol. 11, no. 5, pp. 3871–3884, Sep. 2020.
- [12] X. Zhu, F. Meng, Z. Xie, and Y. Yue, "An inertia and damping control method of DC-DC converter in DC microgrid," *IEEE Trans. Energy Convers.*, vol. 35, no. 2, pp. 799–807, Jun. 2020.
- [13] E. S. N. Raju P. and T. Jain, "A two-level hierarchical controller to enhance stability and dynamic performance of islanded inverter-based microgrids with static and dynamic loads," *IEEE Trans. Ind. Informat.*, vol. 15, no. 5, pp. 2786–2797, May 2019.
- [14] J. Ma, L. Yuan, Z. Zhao, and F. He, "Transmission loss optimization-based optimal power flow strategy by hierarchical control for DC microgrids," *IEEE Trans. Power Electron.*, vol. 32, no. 3, pp. 1952–1963, Mar. 2017.
- [15] S. Sahoo and S. Mishra, "A distributed finite-time secondary average voltage regulation and current sharing controller for DC microgrids," *IEEE Trans. Smart Grid*, vol. 10, no. 1, pp. 282–292, Jan. 2019.
- [16] M. Kordestani, A. A. Safavi, N. Sharafi, and M. Saif, "Novel multi-agent model-predictive control performance indices for monitoring of a large-scale distributed water system," *IEEE Syst. J.*, vol. 12, no. 2, pp. 1286–1294, Jun. 2018.
- [17] F. Perez, A. Iovine, G. Damm, L. Galai-Dol, and P. F. Ribeiro, "Stability analysis of a DC microgrid for a smart railway station integrating renewable sources," *IEEE Trans. Control Syst. Technol.*, vol. 28, no. 5, pp. 1802–1816, Sep. 2020.
- [18] X. Chen, M. Shi, H. Sun, Y. Li, and H. He, "Distributed cooperative control and stability analysis of multiple DC electric springs in a DC microgrid," *IEEE Trans. Ind. Electron.*, vol. 65, no. 7, pp. 5611–5622, Jul. 2018.
- [19] C. Dou, D. Yue, Z. Zhang, and K. Ma, "MAS-based distributed cooperative control for DC microgrid through switching topology communication network with time-varying delays," *IEEE Syst. J.*, vol. 13, no. 1, pp. 615–624, Mar. 2019.
- [20] S. Zuo, T. Altun, F. L. Lewis, and A. Davoudi, "Distributed resilient secondary control of DC microgrids against unbounded attacks," *IEEE Trans. Smart Grid*, vol. 11, no. 5, pp. 3850–3859, Sep. 2020.
- [21] B. Fan, S. Guo, J. Peng, Q. Yang, W. Liu, and L. Liu, "A consensus-based algorithm for power sharing and voltage regulation in DC microgrids," *IEEE Trans. Ind. Informat.*, vol. 16, no. 6, pp. 3987–3996, Jun. 2020.
- [22] B. Fan, J. Peng, Q. Yang, and W. Liu, "Distributed periodic event-triggered algorithm for current sharing and voltage regulation in DC microgrids," *IEEE Trans. Smart Grid*, vol. 11, no. 1, pp. 577–589, Jan. 2020.
- [23] J. Yang, W. Feng, X. Hou, Q. Xia, X. Zhang, and P. Wang, "A distributed cooperative control algorithm for optimal power flow and voltage regulation in DC power system," *IEEE Trans. Power Del.*, vol. 35, no. 2, pp. 892–903, Apr. 2020.
- [24] J. Peng, B. Fan, Q. Yang, and W. Liu, "Distributed event-triggered control of DC microgrids," *IEEE Syst. J.*, to be published, doi: [10.1109/JSYST.2020.2994532](https://doi.org/10.1109/JSYST.2020.2994532).
- [25] S. Abhinav, H. Modares, F. L. Lewis, and A. Davoudi, "Resilient cooperative control of DC microgrids," *IEEE Trans. Smart Grid*, vol. 10, no. 1, pp. 1083–1085, Jan. 2019.
- [26] R. Zhang and B. Hredzak, "Distributed finite-time multiagent control for DC microgrids with time delays," *IEEE Trans. Smart Grid*, vol. 10, no. 3, pp. 2692–2701, May 2019.
- [27] R. Han, H. Wang, Z. Jin, L. Meng, and J. M. Guerrero, "Compromised controller design for current sharing and voltage regulation in DC microgrid," *IEEE Trans. Power Electron.*, vol. 34, no. 8, pp. 8045–8061, Aug. 2019.
- [28] B. Babaiahgari, M. H. Ullah, and J.-D. Park, "Coordinated control and dynamic optimization in DC microgrid systems," *Int. J. Elect. Power Energy Syst.*, vol. 113, pp. 832–841, 2019.
- [29] M. B. Shadmand and R. S. Balog, "Multi-objective optimization and design of photovoltaic-wind hybrid system for community smart DC microgrid," *IEEE Trans. Smart Grid*, vol. 5, no. 5, pp. 2635–2643, Sep. 2014.
- [30] A. Maknouninejad, Z. Qu, F. L. Lewis, and A. Davoudi, "Optimal, nonlinear, and distributed designs of droop controls for DC microgrids," *IEEE Trans. Smart Grid*, vol. 5, no. 5, pp. 2508–2516, Sep. 2014.
- [31] J. Peng, B. Fan, and W. Liu, "Voltage-based distributed optimal control for generation cost minimization and bounded bus voltage regulation in DC microgrids," *IEEE Trans. Smart Grid*, to be published, doi: [10.1109/TSG.2020.3013303](https://doi.org/10.1109/TSG.2020.3013303).

- [32] A. Bracale, P. Caramia, G. Carpinelli, E. Mancini, and F. Mottola, "Optimal control strategy of a DC microgrid," *Int. J. Elect. Power Energy Syst.*, vol. 67, pp. 25–38, 2015.
- [33] Z. Wang, W. Wu, and B. Zhang, "A distributed control method with minimum generation cost for DC microgrids," *IEEE Trans. Energy Convers.*, vol. 31, no. 4, pp. 1462–1470, Dec. 2016.
- [34] S. Moayedi and A. Davoudi, "Unifying distributed dynamic optimization and control of islanded DC microgrids," *IEEE Trans. Power Electron.*, vol. 32, no. 3, pp. 2329–2346, Mar. 2017.
- [35] Z. Wang, F. Liu, Y. Chen, S. H. Low, and S. Mei, "Unified distributed control of stand-alone DC microgrids," *IEEE Trans. Smart Grid*, vol. 10, no. 1, pp. 1013–1024, Jan. 2019.
- [36] B. Fan, Q. Yang, S. Jagannathan, and Y. Sun, "Output-constrained control of nonaffine multiagent systems with partially unknown control directions," *IEEE Trans. Autom. Control*, vol. 64, no. 9, pp. 3936–3942, Sep. 2019.
- [37] R. Semiconductor, "Efficiency of buck converter," *Appl. Note*, Dec. 2016.
- [38] A. P. Ruszczyński and A. Ruszczyński, *Nonlinear Optimization*. Princeton, NJ, USA: Princeton Univ. Press, 2006.
- [39] Y. Zhu, W. Yu, G. Wen, G. Chen, and W. Ren, "Continuous-time distributed subgradient algorithm for convex optimization with general constraints," *IEEE Trans. Autom. Control*, vol. 64, no. 4, pp. 1694–1701, Apr. 2019.
- [40] A. Nedic, A. Ozdaglar, and P. A. Parrilo, "Constrained consensus and optimization in multi-agent networks," *IEEE Trans. Autom. Control*, vol. 55, no. 4, pp. 922–938, Apr. 2010.
- [41] Infineon, "Reverse conducting IGBT with monolithic body diode," IHW50N65R5 datasheet, Dec. 2015.
- [42] S. Peyghami, P. Davari, H. Mokhtari, and F. Blaabjerg, "Decentralized droop control in DC microgrids based on a frequency injection approach," *IEEE Trans. Smart Grid*, vol. 10, no. 6, pp. 6782–6791, Nov. 2019.
- [43] J. P. LaSalle, *The Stability of Dynamical Systems*, vol. 25. Philadelphia, PA, USA: SIAM, 1976.



**Zhen Fan** (Student Member, IEEE) received the B.S. degree in electrical engineering from North China Electric Power University, Baoding, China, in 2017 and the M.S. degree in electrical engineering in 2019 from Lehigh University, Bethlehem, PA, USA, where he is currently working toward the Ph.D. degree in electrical engineering.

His research interests include microgrid, distributed control, renewable energy systems, and power system.



**Bo Fan** (Member, IEEE) received the B.S. degree in automation and the Ph.D. degree in control science and engineering from Zhejiang University, Hangzhou, China, in 2014 and 2019, respectively.

Since 2020, he has been with the Department of Energy Technology, Aalborg University, Aalborg, Denmark, where he is currently a Postdoctoral Researcher. His research interests include distributed control, nonlinear systems, smart grid, and renewable energy systems.



**Jiangkai Peng** (Student Member, IEEE) received the B.Eng. (Hons.) degree in electronics and electrical engineering from The University of Edinburgh, Edinburgh, U.K., and the South China University of Technology, Guangzhou, China, in 2016. He is currently working toward the Ph.D. degree in electrical engineering with Lehigh University, Bethlehem, PA, USA.

His research interests include microgrid, power electronics control system, and power system.



**Wenxin Liu** (Senior Member, IEEE) received the B.S. degree in industrial automation and the M.S. degree in control theory and applications from Northeastern University, Shenyang, China, in 1996 and 2000, respectively, and the Ph.D. degree in electrical engineering from the Missouri University of Science and Technology (formerly University of Missouri–Rolla), Rolla, MO, USA, in 2005.

From 2005 to 2009, he was an Assistant Scholar Scientist with the Center for Advanced Power Systems, Florida State University, Tallahassee, FL, USA.

From 2009 to 2014, he was an Assistant Professor with the Klipsch School of Electrical and Computer Engineering, New Mexico State University, Las Cruces, NM, USA. He is currently an Associate Professor with the Department of Electrical and Computer Engineering, Lehigh University, Bethlehem, PA, USA. His research interests include power systems, power electronics, and controls.

Dr. Liu is an Editor of the *IEEE TRANSACTIONS ON SMART GRID*, *IEEE TRANSACTIONS ON POWER SYSTEMS*, and *Journal of Electrical Engineering & Technology*, and an Associate Editor for the *IEEE TRANSACTIONS ON INDUSTRIAL INFORMATICS*.